Advances in the Estimation of Ice Particle Fall Speeds Using Laboratory and Field Measurements

A. J. HEYMSFIELD

NCAR, Boulder, Colorado

C. D. WESTBROOK

Department of Meteorology, University of Reading, Reading, United Kingdom

(Manuscript received 13 November 2009, in final form 19 March 2010)

ABSTRACT

Accurate estimates for the fall speed of natural hydrometeors are vital if their evolution in clouds is to be understood quantitatively. In this study, laboratory measurements of the terminal velocity v_t for a variety of ice particle models settling in viscous fluids, along with wind-tunnel and field measurements of ice particles settling in air, have been analyzed and compared to common methods of computing v_t from the literature. It is observed that while these methods work well for a number of particle types, they fail for particles with open geometries, specifically those particles for which the area ratio A_r is small (A_r is defined as the area of the particle projected normal to the flow divided by the area of a circumscribing disc). In particular, the fall speeds of stellar and dendritic crystals, needles, open bullet rosettes, and low-density aggregates are all overestimated. These particle types are important in many cloud types: aggregates in particular often dominate snow precipitation at the ground and vertically pointing Doppler radar measurements.

Based on the laboratory data, a simple modification to previous computational methods is proposed, based on the area ratio. This new method collapses the available drag data onto an approximately universal curve, and the resulting errors in the computed fall speeds relative to the tank data are less than 25% in all cases. Comparison with the (much more scattered) measurements of ice particles falling in air show strong support for this new method, with the area ratio bias apparently eliminated.

1. Introduction

The sedimentation rates of ice crystals and snowflakes remain poorly characterized at present. Analytical solutions for the terminal velocity v_t of natural ice particles as they fall through the air have not been forthcoming because of their nonspherical shape and the range of flow regimes that they span. Empirical formulas based on experimental data and approximate theory are therefore required to predict how fast an ice particle with a given shape, size, and mass will fall. This is often achieved using a relationship of the form

$$v_t = \alpha D^{\beta}, \tag{1}$$

where D is the maximum dimension of the particle, and the constants α and β have been measured for a variety of particle habits at the ground (e.g., Locatelli and Hobbs 1974). Such relationships are used to parameterize cloud, numerical weather prediction, and climate models (e.g., Rutledge and Hobbs 1984; Wilson and Ballard 1999). However, it is clear that these relationships are specific to the ice particles for which they were measured. This is illustrated in Fig. 1, which shows the fall speed measured for aggregate snowflakes a few millimeters in size falling from different clouds. In the first dataset [dense aggregates of complex polycrystals from Locatelli and Hobbs (1974)] the particles fell at $\sim$1.2 m s^{-1}. In the second dataset [open aggregates of dendritic crystals from Kajikawa (1982)], particles of the same size were observed to sediment at only $\sim$0.4 m s^{-1}. Although in both cases the particles were classified as aggregates, there were obviously significant differences in the particle properties to have such different fall speeds. It is therefore extremely desirable to explicitly factor the particle mass and shape into fall speed calculations.

Corresponding author address: Dr. Andrew Heymsfield, NCAR, P.O. Box 3000, Boulder, CO 80307–3000.
E-mail: heyms1@ucar.edu

DOI: 10.1175/2010JAS3379.1

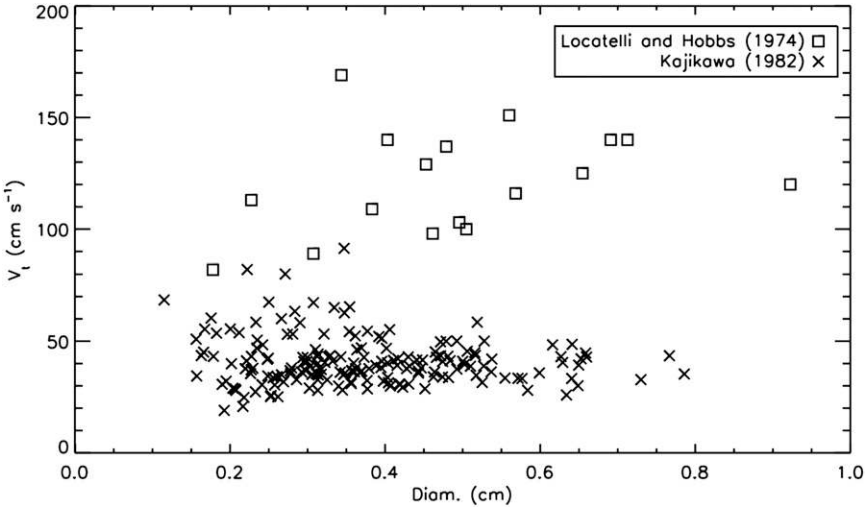

FIG. 1. Measured fall speed of aggregate snowflakes as a function of D composed of different component crystal types (see text for details).

This motivated Böhm (1989, 1992),[1] Mitchell (1996), Mitchell and Heymsfield (2005), and Khvorostyanov and Curry (2002, 2005) to propose fall speed relationships based not only on D but also on the particle's mass m and area A projected normal to the fall motion. It seems intuitively sensible to expect the fall speed to depend primarily on these three parameters; however, there is a need to test these formulas and to understand their strengths and weaknesses. Westbrook (2008) noted that the latter four studies (from now on collectively referred to as MHKC) overestimate the fall velocity of sub-100-μm crystals, particularly when the particle geometry is open.

In what follows we use a number of experimental datasets in which the most important variables are measured rather than estimated to test the methods cited. These datasets may be divided into two groups: 1) laboratory tank measurement of the drag on model ice crystal and aggregate shapes falling through viscous liquids and 2) observations of real ice particles falling through the atmosphere. Both datasets have their advantages and drawbacks. In the first group, the experimental errors are very small (~10%) but a relatively small range of idealized shapes is sampled. The data in the second group are subject to much larger experimental errors because of the challenge of measuring m, A, D, and v_t simultaneously in the field; however, the range of particle properties is much broader, which therefore gives us confidence that the conclusions drawn from the tank experiment comparisons are generally applicable to natural ice particles.

The article is organized as follows. In section 2 we review the relevant drag parameters and theoretical background for spherical particles. The results of MHKC are then tested against the data from groups 1 and 2, and their relative strengths and weaknesses are identified. Having identified a specific weakness in the MHKC methods, we propose a simple modification to the Re–X formula of Mitchell (1996), which leads to much improved agreement with the laboratory and observational data but is equally straightforward to apply.

2. Background

Conventionally the drag on a falling particle is expressed in terms of a dimensionless drag coefficient C_d:

$$F_d = \frac{1}{2}\rho_{\text{air}} v_t^2 A C_d, \tag{2}$$

where ρ_{air} is the density of the air and F_d is the drag force. In general, C_d is a function of the Reynolds number $\text{Re} = \rho_{\text{air}} v_t D/\eta$, where η is the dynamic viscosity of the air. For calculation of terminal velocities, the Davies or Best number $X = C_d\text{Re}^2$ is helpful, since Eq. (2) with the drag force set equal to the weight of the particle mg, where g is gravity, yields the result

$$X = \frac{\rho_{\text{air}}}{\eta^2}\frac{2mgD^2}{A}. \tag{3}$$

[1] Böhm's (1989, 1992) methods rely on the ice particle being approximated by an equivalent spheroid that must be classed as prolate or oblate. Since it is not possible to classify many natural ice particles (e.g., irregular polycrystals and aggregates) in this manner, we have not applied Böhm's equations in this study.

In other words, X may be calculated from the known properties of the ice particle (m, A, D) and the air (ρ_{air}, η) but does not depend on v_t. The task then is to relate X to Re (or equivalently C_d to Re), so that for a given ice particle and environmental conditions X can be computed directly, Re can be estimated from X, and thus the fall speed is known: $v_t = \eta \text{Re}/D\rho_{\text{air}}$.

a. Spherical particles

It is instructive to review the behavior of spherical particles, since we may anticipate that the drag on nonspherical ice particles is likely to take a similar form, albeit with altered parameters (Mitchell 1996). Importantly, Abraham (1970) viewed the problem in terms of an ''assembly'' of the particle plus an attached boundary layer. The drag was then taken to be the inviscid (large Re) drag on the complete assembly. It is well known (Batchelor 1967) that the average depth of this boundary layer is $\delta = \delta_0 D/\sqrt{\text{Re}}$, where δ_0 is a dimensionless coefficient. Hence, the effective area of the assembly is increased by a factor $(1 + \delta/D)^2$ compared to the area of the sphere, $A = \pi D^2/4$, alone. This leads to a drag coefficient for the particle:

$$C_d = C_0\left(1 + \frac{\delta_0}{\sqrt{\text{Re}}}\right)^2, \tag{4}$$

where C_0 is the inviscid drag coefficient for the assembly (assumed constant). The corresponding Re–X relationship (Böhm 1989) is

$$\text{Re} = \frac{\delta_0^2}{4}\left[\left(1 + \frac{4\sqrt{X}}{\delta_0^2\sqrt{C_0}}\right)^{1/2} - 1\right]^2. \tag{5}$$

McDonald (1954) estimated $\delta_0 \approx 9.06$ for water drops, and Abraham (1970) finds that choosing $C_0 = 0.292$ is an excellent fit to the experimental data for smooth spheres when $\text{Re} < 10^4$. Abraham also observed that Eq. (5) is consistent with experimental data even for low Reynolds numbers where the boundary layer concept breaks down, as well as Stokes' analytical solution in the limit $\text{Re} \to 0$.

b. Nonspherical particles

For nonspherical particles a number of measurements have been made of terminal velocity of model particles in the laboratory and the natural particles in the field. From these velocities and from measurements of m, A, D, ρ_{air}, and η, empirical C_d(Re)–Re(X) curves may be derived. These measurements are described in more detail in the next section. The purpose of the MHKC studies, and the present work, is to modify Abraham's method in order to find a single equation that accurately describes all of the available C_d(Re) data for different particle shapes.

3. Evaluation of MHKC methods

The method described by Mitchell (1996) is the most widely cited and also the simplest. Essentially it is assumed that a single C_d(Re) or Re(X) relationship is sufficient to describe all natural ice particles. Equations (4) and (5) are simply applied with altered coefficients: $C_0 = 0.6$, $\delta_0 = 5.83$. To facilitate the discussion that follows, we introduce the area ratio of the particle A_r, which is the ratio of the particle's projected area A to the area of a circumscribing circle, $A_r = A/[(\pi/4)D^2]$. This fraction varies between 0 and 1 depending on the particle shape. Note that in this paper we define D as the maximum dimension of the particle's projection normal to the direction of fall (rather than maximum span in three dimensions).

The Best number inserted into Eq. (5) is therefore

$$X = \frac{\rho_{\text{air}}}{\eta^2}\frac{8mg}{\pi A_r}. \tag{6}$$

For numerical convenience Mitchell (1996) split the continuous curve [Eq. (5)] into four approximately linear sections on a log Re–log X diagram, facilitating the generation of v_t–D power-law-type relationships of the form given by Eq. (6). Khvorostyanov and Curry (2002) took this approach one stage further by recasting Eq. (5) as a power law with continuous variable coefficients. Mitchell and Heymsfield (2005) introduced a turbulent correction to increase the drag at very large Re. Khvorostyanov and Curry (2005) used an alternative approach to introduce this extra turbulent drag. Khvorostyanov and Curry's (2005) curve is plotted as a dashed line in Fig. 2 and over the range of Reynolds numbers considered ($1 < \text{Re} < 1000$) it is essentially indistinguishable from that of Mitchell (1996). Mitchell and Heymsfield's (2005) empirical correction has a more significant effect and acts to increase the drag somewhat as shown in Fig. 2 (dashed line). At Reynolds numbers less than ~100 all three methods may be considered identical.[2]

[2] Khvorostyanov and Curry (2002) used Abraham's values of C_0 and δ_0 instead of the ones detailed above but changed them to match Mitchell's choice in their 2005 paper after comments by Mitchell and Heymsfield (2005). For brevity, we have not considered their 2002 study in our comparison.

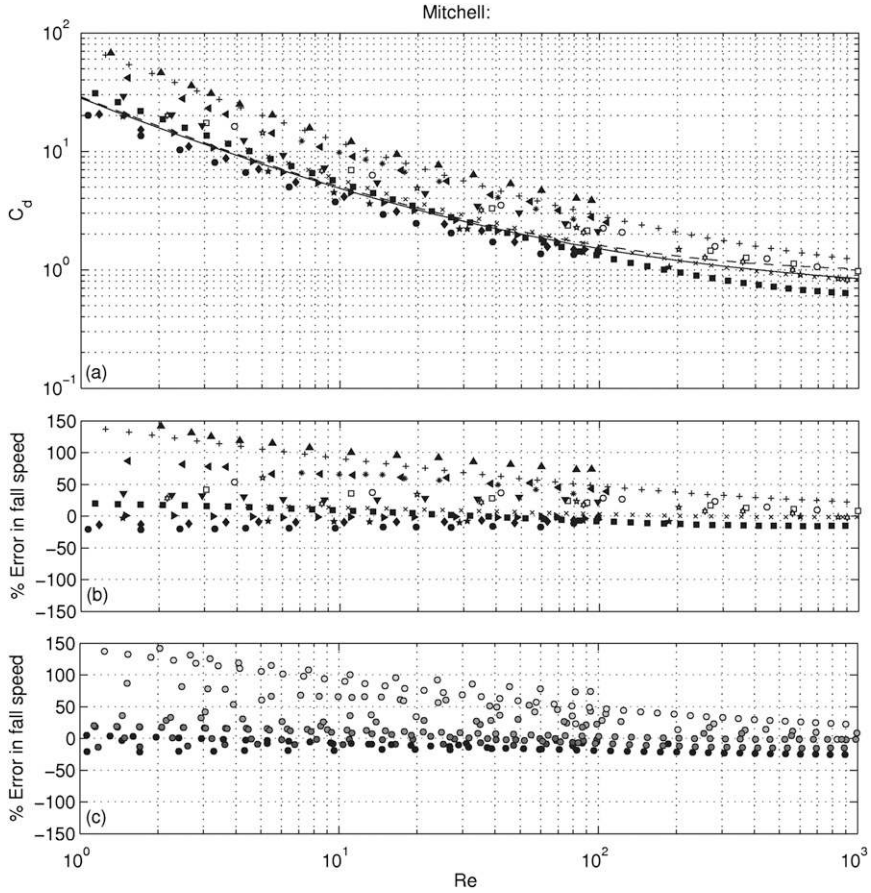

FIG. 2. Tank experiment data. (a) Comparison of experimental Re–X data (symbols) with theoretical curve of Mitchell (1996; solid line), Mitchell and Heymsfield (2005; dashed line), and Khvorostyanov and Curry (2005; dotted line). (b) Corresponding relative error in fall speed for a given Re if Mitchell's curve is assumed. (c) As in (b), but symbols are now replaced by circles filled with different shades of gray, with darker shades symbolizing larger A_r ($A_r = 1$ is black and $A_r = 0$ is white). Symbols in (a) and (b) are as follows. Planar types are filled: disc is a circle, hexagonal plate is a diamond, broad-branch crystal is a right-pointing triangle, plate with extensions is a down-pointing triangle, dendrite is a left-pointing triangle, and stellar is an up-pointing triangle. Thick disc (aspect ratio 0.5) is a black pentagram. Cylinders with aspect ratio: 10 is a plus sign, 5 is an asterisk, 2 is an ex, and 1 is a black filled square. Aggregates are open: cross shape is a circle, H shape is a square, star shape is a hexagram, and chain is a pentagram. See text for more details.

a. Laboratory data: Model ice particles

In addition to the MHKC curves, Fig. 2 also shows experimental data from a variety of tank experiments. It is immediately apparent that there is a very large spread in the drag coefficient for a given Re as the particle shape is changed. The individual datasets are described below.

List and Schemenauer (1971) have measured C_d(Re) for a variety of planar ice crystal shapes up to Re ~100. The ice crystal shapes used are illustrated in Fig. 3; all the models were made of metal with an aspect ratio (thickness divided by maximum span in the basal plane) of 0.02 and were dropped in tanks of salt solutions or glycerin and water mixtures. These data are shown in Fig. 2a. Also plotted, in Fig. 2b, is the corresponding error in the Reynolds number (and therefore also in v_t) if Re is calculated from Eq. (5) using the coefficients from Mitchell (1996). These data show that thin circular discs ($A_r = 1$), hexagonal plates ($A_r = 0.83$), and broad branched crystals ($A_r = 0.74$) are all well approximated by Mitchell's approach, with errors in the computed fall speed of ≤20%. As the crystals become more tenuous and complex in their projection, Mitchell's curve is observed to increasingly overestimate v_t, the most extreme case being the stellar crystal that had $A_r = 0.185$: here

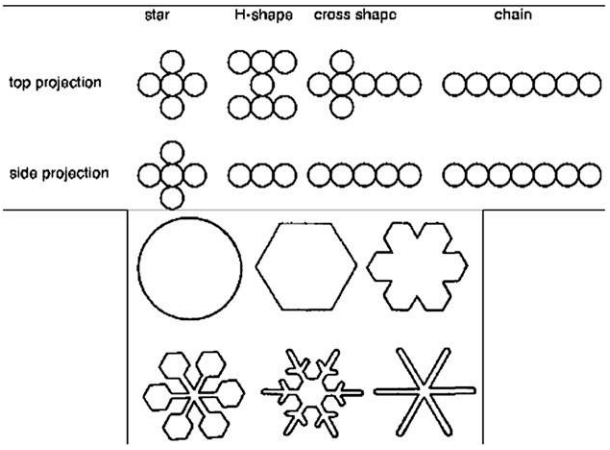

FIG. 3. Ice crystal models. (top) Aggregates of spheres measured by Tran-Cong et al. (2004); (bottom) planar crystals used by List and Schemenauer (1971).

errors in excess of 100% were found for Reynolds numbers <10. Dendrites ($A_r = 0.28$) also led to substantial errors of 40%–80% depending on Re. The stellar with end plates model with $A_r = 0.47$ had much more modest errors of 20%–35%. We note that List and Schemenauer (1971) remarked on the large difference in drag coefficient between a solid disc and the more tenuous dendrites and stellars. They suggested an empirical formula to describe all their models in terms of the drag on a disc, with a correction factor based on A_r.

We note that Jayaweera (1972) suggested that the terminal velocity of planar crystals could be approximated by that of a circular disc of the same mass and thickness, based on model tank experiments similar to those of List and Schemenauer. In this case, the velocity of open stellar crystals was measured to be only 25% lower than those of circular discs. At first sight this seems at odds with the rather strong dependence of C_d(Re) on area ratio reported above. However, consider two models with equal mass and thickness. Model A is a disc $A_r = 1$ and model B is a stellar $A_r = 0.2$; both are measured to have similar velocities. In this case, since m is proportional to A, the two models must also have the same C_d because of Eq. (4). So C_d is the same for a given velocity v_t. But D of the stellar model is a factor of $\sqrt{5}$ larger than that of the disc: this means that the Reynolds number of the stellar crystal $\mathrm{Re} = \rho_{\mathrm{air}} v_t D/\eta$ is larger by the same factor. In other words, C_d is being measured at different Re for the different models, and therefore they do *not* follow the same C_d(Re) curve. This is an important distinction to make. If the mass and thickness of the planar crystal is known, Jayaweera's result is certainly a useful rule of thumb.

Jayaweera and Cottis (1969) and Kajikawa (1971) have investigated the sedimentation of circular cylinders in a similar manner to List and Schemenauer (1971). There is some overlap between their data, and for simplicity we show only the results from Jayaweera and Cottis for cylinders of aspect ratio 1, 2, and 10. Kajikawa (1971) reports additional results for aspect ratio = 5, and these data are included in our analysis. Podzimek (1965) has shown that the drag on hexagonal columns is very similar to that on circular cylinders of the same aspect ratio. The Re–X data are plotted in Fig. 2a and associated errors in Fig. 2b as before. The cylinders all fell preferentially with their major (c) axis horizontal. We observe that for short columns (aspect ratio = 1, 2) Mitchell's formula performs well, with errors in the calculated fall velocity less than 20%. For longer columns, with aspect ratio = 5 the errors are larger (30%–70%), while for long needles errors in excess of 100% can be expected for Reynolds numbers <20. Such crystals grow readily at temperatures close to −5°C, and accurate estimates of their sedimentation velocity are likely to be important for quantitative modeling of the Hallett–Mossop process (Pruppacher and Klett 1997).

Aggregation is an important process in both cirrus and deep precipitating frontal systems (Field and Heymsfield 2003; Pruppacher and Klett 1997), and indeed the majority of particles sampled in snowfall at the ground are aggregates (Hobbs et al. 1974). However, these particles remain poorly characterized, and there is very little quantitative data available. To the authors' knowledge, no systematic measurements of the drag on models of ice crystal aggregates have been made. As an approximation to ice aggregates, we have analyzed the data presented by Tran-Cong et al. (2004), who connected spheres in various configurations to produce simple aggregate particles and measured their settling velocity in glycerin–water mixtures. Seven spheres were used to make each of the four aggregate configurations analyzed here (see Fig. 3). Although these models are much simplified relative to natural snowflakes, they would seem to be a logical first test of any theory of aggregate fall speeds.

The C_d(Re) data and relative errors in fall speed when Mitchell's curve is assumed are plotted in Figs. 2a,b as before (white filled symbols). We observe that the predicted fall speeds are too large relative to the experimental data, by as much as 60% for the chainlike aggregate. Geometries similar to these have been observed in thunderstorms (Stith et al. 2004; see also Connolly et al. 2005 and references therein). The more complex aggregate geometries show that errors between 10% and 50% may be expected, with larger errors at lower Re. Area ratios for these particles were 0.55 for the star, 0.39 for the H shape, 0.28 for the cross, and 0.14 for the linear chain.

Finally, we have replotted Fig. 2b, this time marking each data point as a circle in Fig. 2c, where the shading indicates the area ratio (black for $A_r = 1$, white for $A_r = 0$).

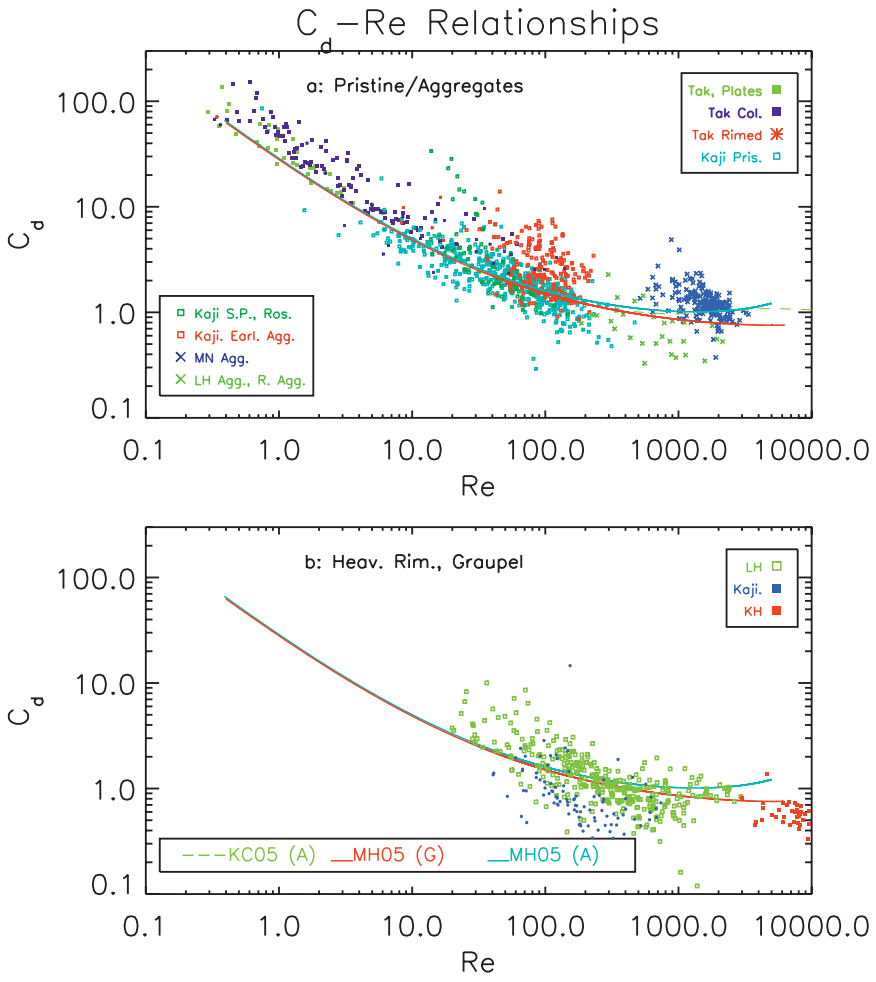

FIG. 4. The C_d derived from measurements of ice particle v_t, m, and A from the studies in section 3b compared to the MHKC curves. (a) Pristine and lightly rimed particles; (b) heavily rimed particles and graupel.

The stratification of data in this plot is revealing: errors in v_t are small for particles where A_r is close to 1; as A_r becomes smaller the terminal velocity is increasingly overestimated.

b. *Measurements of ice crystals falling in air*

We now make the same comparison using measurements of ice particles falling in air. Drag coefficients, derived from Eq. (1) for each of the particles in the following data samples, are plotted as a function of Re in Fig. 4.

The fall velocities of single crystals have been measured for laboratory and naturally grown crystals. Properties of 511 various planar crystal habits in different stages of riming were reported in Heymsfield and Kajikawa (1987). Maximum dimensions ranged from 250 μm to 6.5 mm; area ratios varied from 0.3 to 1. Takahashi and Fukuta (1988) and Takahashi et al. (1991) measured m, D, and A for 226 planar and columnar-type ice crystals nucleated and grown for periods of up to 30 min at constant temperature (between −3° and −23°C) while held freely suspended in a vertical supercooled cloud tunnel, while v_t was determined from the airspeed. Maximum dimensions spanned the range from approximately 75 μm to 4 mm: many of the larger particles were rimed. Figure 4 shows the derived drag coefficients of these crystals: most are higher than predicted by MHKC. Heymsfield and Iaquinta (2000) reported on the properties and fall speeds of 79 side planes, capped columns, and bullet rosettes measured at the ground by M. Kajikawa. Maximum dimensions ranged from 400 μm to 2 mm.

Although the data in Fig. 4a show a broad scatter, we can see that the drag measured for the side plane and rosette crystals is significantly higher than predicted by MHKC. These particles were among the most open in the datasets shown here, with area ratios in the range of 0.2–0.4, and we interpret this as evidence of the

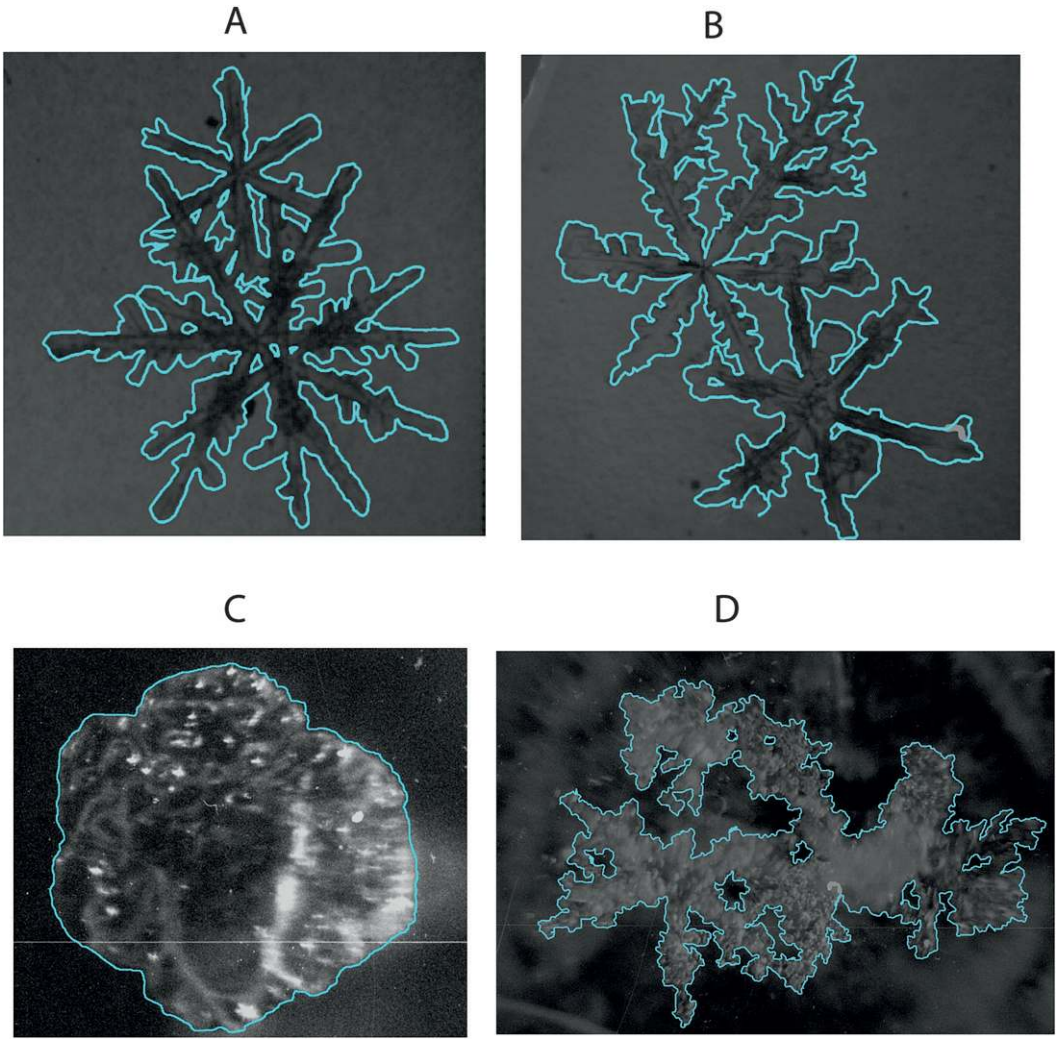

FIG. 5. Examples of traced images of (a),(b) early aggregates, $D = 4.8$, 4.6 mm, from the Kajikawa (1982) early aggregate study, and (c),(d) a 0.9-mm graupel particle and a 4.7-mm aggregate from the Locatelli and Hobbs (1974) collections.

oversensitivity of the MHKC approach to A_r observed in the tank data comparison. (This can be observed in better detail in Fig. 7, which shows the deviation relative to Mitchell and Heymsfield's drag curve.) The drag on the pristine column and platelike crystals measured in Takahashi's experiments is also consistently higher than or equal to that predicted by the MHKC curves. Kajikawa's planar crystal drag coefficients are quite scattered: these data are largely clustered around the MHKC curve.

The data for aggregates are less comprehensive than for single crystals. Kajikawa (1982) measured the fall behavior and velocity of 188 early aggregates containing 2–6 component crystals, with sizes ranging between approximately 1 and 8 mm. We have digitized and traced these particles and derived the particle area ratios using Kajikawa's high-quality photographs (e.g., Figs. 5a,b). Maximum diameters ranged from 1 to 8 mm. These particles had very open ''fluffy'' geometries, and area ratios were in the range of 0.15–0.55. Like the rosette and side plane data points, the drag coefficients of these particles are substantially higher than predicted by MHKC by 100% or more in a number of cases (Fig. 4a); again, we argue that this is because of their low area ratios, and this is further evidence for the oversensitivity of the MHKC method to A_r observed in the tank data comparison.

Heymsfield et al. (2002) reported on the reanalysis of data (v_t, m, and A_r) for 185 aggregates measured by Magono and Nakamura (1965). The particle sizes ranged from 6 to 30 mm and the masses were measured directly; X and Re could then be derived. We note that Magono and Nakamura (1965) essentially estimated the particle area ratio by eye, and this introduces some

uncertainty into the estimated values of C_d. The drag coefficient of these very large aggregates is significantly higher than that predicted by Mitchell (1996). The correction term used by Mitchell and Heymsfield (2005) for aggregates was developed based on this dataset, and it is therefore no surprise that their curve is a rather better approximation for these particles than that of Mitchell (1996).

The fall velocity of heavily rimed particles and graupel has been measured in a few studies. Locatelli and Hobbs (1974) reported on the fall speed and dimensions of more than 400 particles—mostly heavily rimed crystals and graupel but with some aggregates, at sizes ranging from 500 μm to almost 1 cm. We digitized the original photographs to find the maximum dimension and cross-sectional areas of those particles: examples of these particles are shown in Figs. 5c,d. Heymsfield and Kajikawa (1987) and Knight and Heymsfield (1983) reported on the properties of 400 graupel particles, some exceeding 1 cm in diameter, which were collected at the ground at temperatures near 0°C. For both studies, a mean diameter was derived, yielding approximately the correct cross-sectional area but D and A_r were not measured. Derived C_d values are therefore accurate but Re might be overestimated by a mean of approximately 20% if we consider the ratio of the mean to maximum diameter from the other studies. We find that the data approximately follow Mitchell's (1996) drag law for graupel (Fig. 4, red curve). Note that if Mitchell and Heymsfield's (2005) turbulent correction for aggregates is applied to Knight and Heymsfield's very large graupel particles, the computed drag is overestimated by approximately 50% (see Fig. 4b).

The drag coefficient measurements above suggest a similar behavior to that observed in the tank experiments. To investigate this in more detail we have plotted the ratio of the predicted to the measured fall speed for all of the particles as a function of both size and A_r (shown in Figs. 6a–d). The comparison shows that on average the predicted fall speed is well captured as a function of size; however, this median ratio is weighted by the distribution of particle shapes present in the dataset. When plotted as a function of area ratio, a clear bias is observed, with particle fall speeds that are too fast at low A_r and too slow at high A_r. This therefore adds weight to the argument put forward in section 3a.

c. Discussion

Comparison of the MHKC methods with tank experiments, wind tunnel data, and field measurements of natural ice particles strongly suggests that the fall speed of particles with low area ratios are overestimated, in some cases by 100% or more; this effect appears to be strongest at lower Re (Fig. 7). Needles, dendrites, stellars, and aggregates are key particle types that are affected by this bias. Compact particles with high area ratios such as rimed particles and graupel, on the other hand, appear to be well captured by Mitchell's (1996) curve. The corrections at Re $\gg$ 100 proposed by Khvorostyanov and Curry (2005) and Mitchell and Heymsfield (2005) bring the data more into line with the very large snowflakes measured by Magono and Nakamura; however, the prediction of v_t for the early aggregates of Kajikawa is not improved by this empirical correction, which does not account for the observed variation in C_d(Re) with A_r. We believe a modification of the MHKC approach is necessary to capture this dependence.

4. A new approach

In this section, we propose a simple adjustment to Mitchell's (1996) formula, which leads to a much improved agreement with the available data. Given that the fall speed calculated by Mitchell's method is observed to be too sensitive to A_r, we consider a modified drag coefficient of the form

$$C_d^* = C_d A_r^k \tag{7}$$

and a corresponding modified Best number:

$$X^* = \frac{\rho_{\text{air}}}{\eta^2}\frac{8mg}{\pi A_r^{1-k}}. \tag{8}$$

We then simply adjust the value of $0 \le k \le 1$ until the laboratory data points collapse onto a single curve (or fit a single curve as closely as possible). After experimentation using Eq. (7) we find that $k = 0.5$ provides optimum agreement with the available data. This is illustrated in Fig. 8; compare this to the spread of data points in Fig. 2. Like Mitchell's approach, our method requires knowledge only of m, A, and D and does not draw a distinction between "prolate" and "oblate" particle types, nor does it require knowledge of particle aspect ratios.

We have fitted a curve of the form given by Eq. (4) to the renormalized data and estimate the fitting parameters $C_0 = 0.35$ and $\delta_0 = 8.0$. Figure 8 shows this curve alongside the experimental data. Also shown in the figure are the relative errors in the computed fall speed when the new method is applied: in all cases this error is 25% or less. This is good evidence that our proposed method has a realistic sensitivity to A_r.

The procedure for calculating v_t using this new method is as follows:

1) Given η, ρ_{air}, m, A_r, and D, calculate the modified Best number:

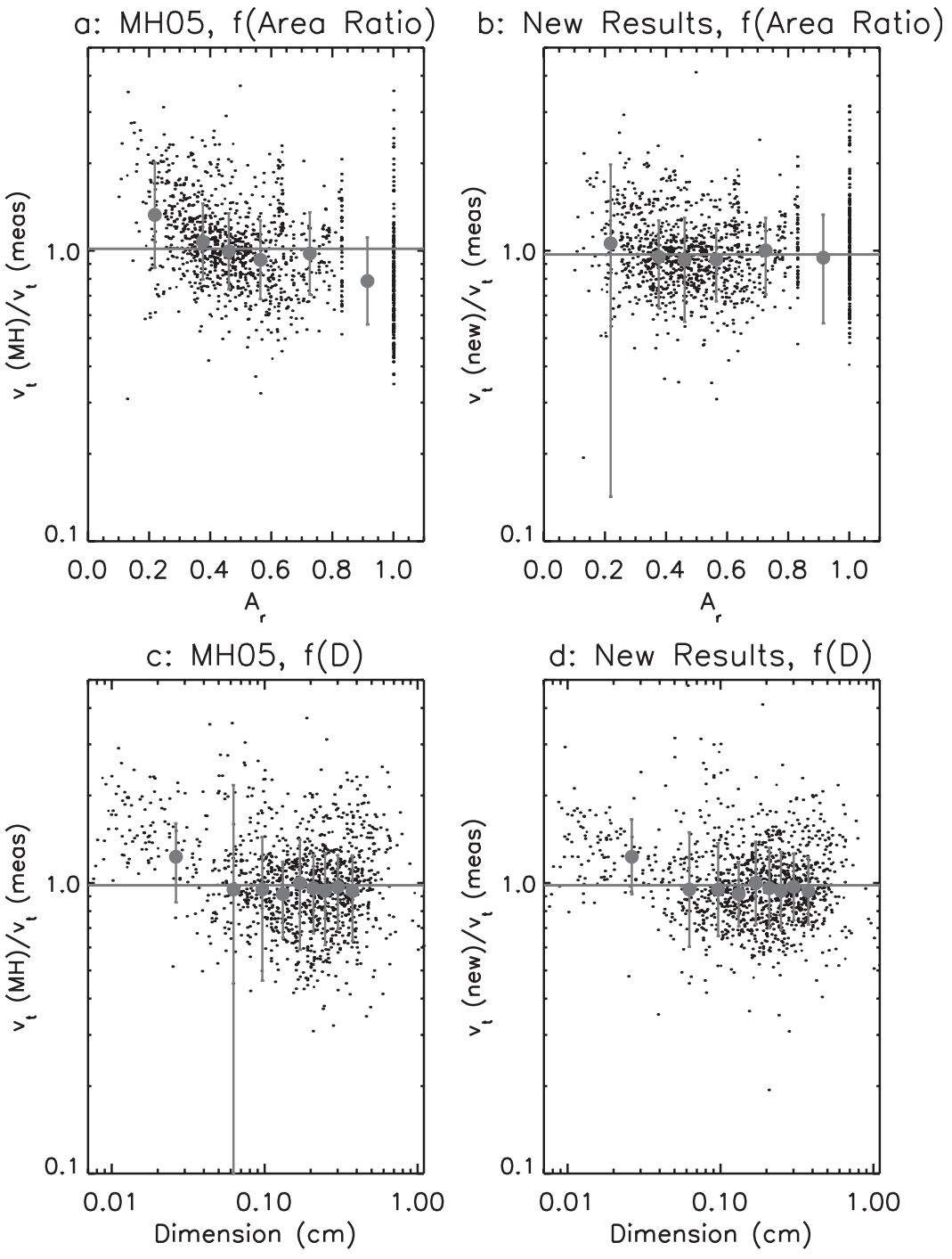

FIG. 6. Comparison of v_t of ice crystals falling in air with that predicted by Mitchell and Heymsfield (2005) and the new computational method, plotted as a function of (a),(b) A_r and (c),(d) D. In each panel, mean values and standard deviations are shown with points and bars, respectively; the median value for all data points is shown by horizontal line. Few observations are for $D > 2$ cm; the abscissa is therefore truncated.

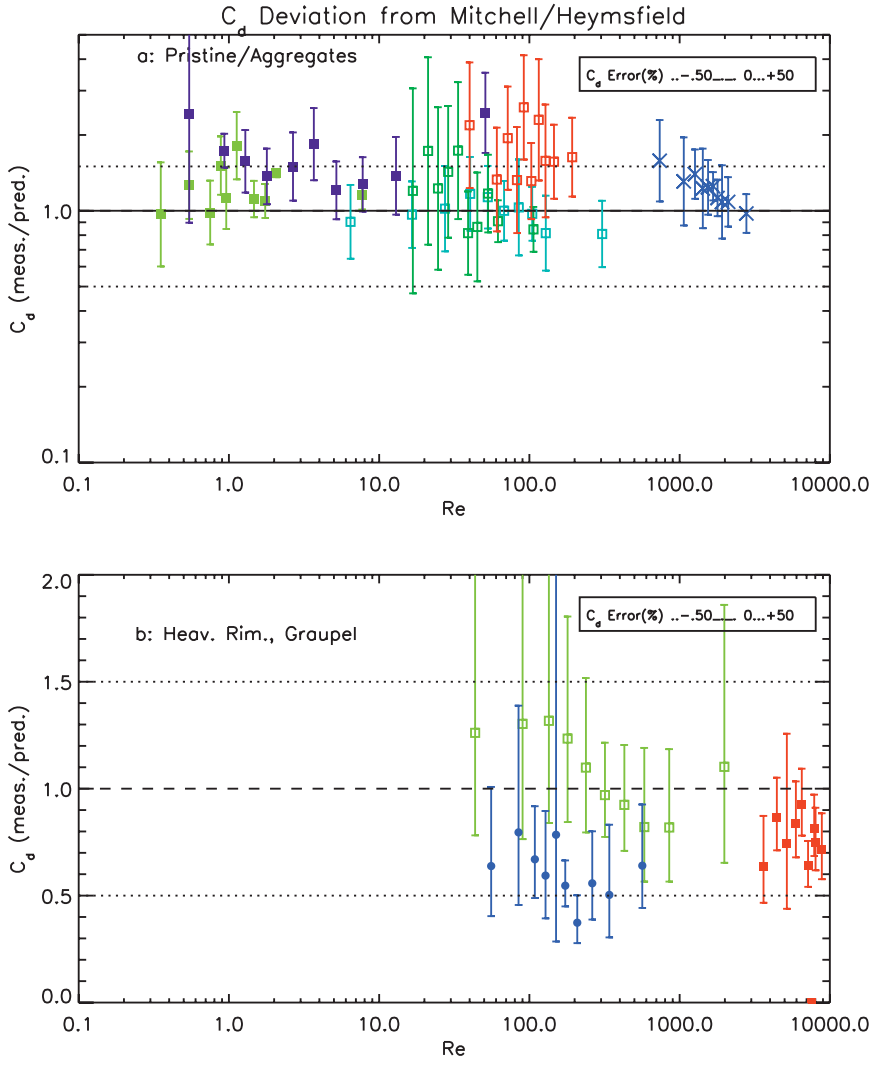

FIG. 7. Ratio of C_d derived from measurements to C_d derived from the Mitchell and Heymsfield (2005) relationship for (a) pristine particles and (b) heavily rimed ice and graupel, with color codes as given in Figs. 4a,b). Note the scale change between panels. Horizontal lines denote specific errors in C_d.

$$X^* = C_d^* Re^2 = \frac{\rho_{\text{air}}}{\eta^2}\frac{8mg}{\pi A_r^{0.5}}.$$

2) From this the Reynolds number is estimated:

$$\text{Re} = \frac{\delta_0^2}{4}\left[\left(1 + \frac{4\sqrt{X^*}}{\delta_0^2\sqrt{C_0}}\right)^{1/2} - 1\right]^2$$

using $C_0 = 0.35$ and $\delta_0 = 8.0$.

3) Finally the fall speed is computed directly:

$$v_t = \frac{\eta \text{Re}}{\rho_{\text{air}} D}.$$

a. Comparison with ice crystals falling in air

In Fig. 6, we compare the terminal velocity measurements described in section 3b to those calculated using the new approach. The ratio of the predicted and measured terminal velocity is plotted as a function of area ratio (Fig. 6a,b) and also as a function of size (Fig. 6c,d) for the relationship given in Mitchell and Heymsfield (2005) and the new relationships. There is substantial scatter in all diagrams, and this probably reflects the challenge of making accurate measurements of v_t, m, A, and D simultaneously in the field. In particular, A and v_t may even vary in time if the particles are not stable as they fall; characterization of such behavior is particularly difficult. However, Fig. 6 shows that *on average*

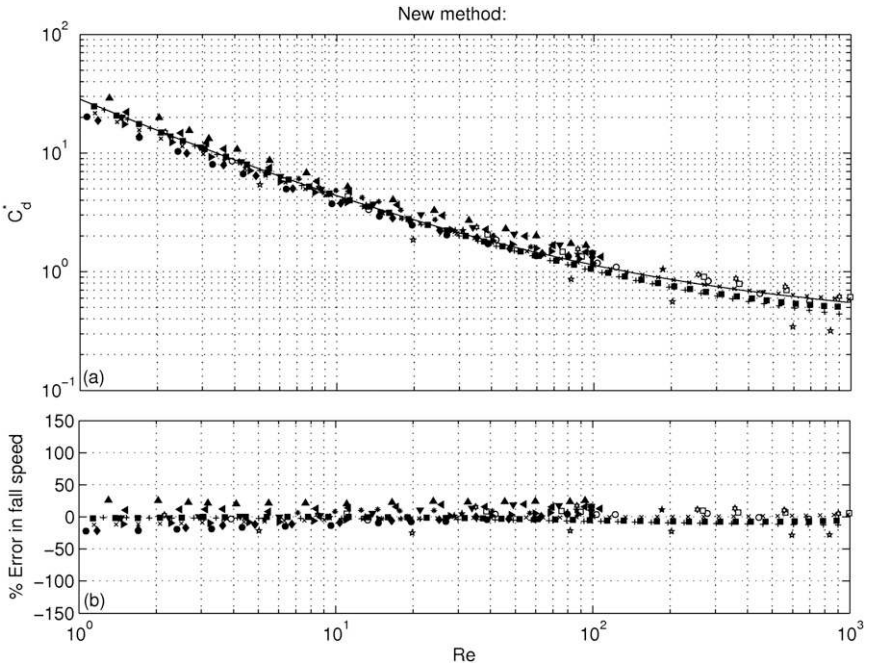

FIG. 8. Plots of (a) C_d^* with $k = 0.5$ and (b) relative error in v_t calculated using the new method. Symbols are as in Fig. 2.

the new method gives a predicted v_t that is very close to that which is measured, and the ratio of the two does not have any clear variation with either D or A_r (unlike MHKC). The scatter in the data when plotted as a function of A_r is also slightly reduced, which may be evidence that our method is effective at collapsing the data for a range of shapes. These measurements give us confidence that the method is likely to be quite robust.

Graupel data from Heymsfield and Kajikawa (1987) and Knight and Heymsfield (1983) did not include A_r and only the mean diameter was reported, and for those reasons graupel data are not plotted in Fig. 6. As a first approximation we can assume that the area ratios of the graupel are 0.8 (based on our analysis of other datasets). With that assumption, the ratio of calculated to measured v_t for the 333 Heymsfield and Kajikawa graupel particles is a mean of 0.91 ± 0.25; for the 37 Knight and Heymsfield graupel particles it is 0.97 ± 0.11.

b. Comparison with the Westbrook (2008) study

Most of the data analyzed here has $\mathrm{Re} > 1$; however, the smallest particles in clouds can fall in a purely viscous regime. This was explored using theoretical arguments and experimental data (from cold room experiments) by Westbrook (2008). We now briefly investigate how the new method proposed above compares to his results for small (sub-100 μm) crystals.

For small Re our new method reduces to

$$v = \frac{g}{6\pi\eta}\frac{m}{R}, \tag{9}$$

where the "hydrodynamic radius" R controlling the drag is

$$R = 0.465 D A_r^{0.5}. \tag{10}$$

For a simple sphere $A_r = 1$ and our new method reproduces the Stokes solution for a sphere to within 7%. Westbrook (2008) estimated R for hexagonal plates, branched crystals, and columns. A calculation was also made for bullet rosettes; however, this was purely theoretical because of the lack of experimental data available. In all cases R was closely related to the "capacitance" C, a length scale characterizing the diffusion of momentum from the crystal.

At low Re crystals may be oriented quasi-randomly, and we have calculated the fall velocity assuming both horizontal and random orientation. For all crystal types and for both horizontal and random orientation we find that the computed fall velocities using the new method are within ~30% of Westbrook's (2008) data, giving us confidence that our new method may be applied even for $\mathrm{Re} < 1$. The reduced sensitivity of the computed drag force to A_r compared to the MHKC approach seems to make the estimates of v_t much more reliable in this regime. More experimental data for $\mathrm{Re} < 1$ is highly desirable, however,

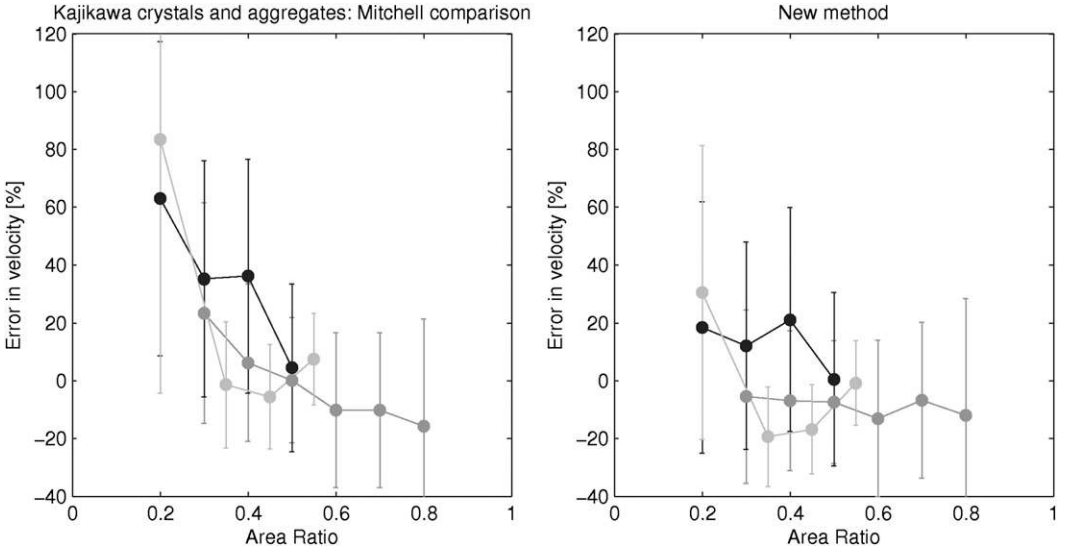

FIG. 9. (left) Percentage error in v_t calculated for Kajikawa's single planar crystals (dark gray), bullet rosettes and side planes (light gray), and early aggregates (black) using Mitchell's (1996) method. (right) As at left, but using the new method (see text). Data points represent median error over A_r bins of width 0.1, except for the light gray point at $A_r = 0.2$ for which the bin width was 0.2. Error bars show 1 std dev. All bins contained at least 10 particles.

particularly for more complex particles such as rosettes and other polycrystals in the early stages of growth.

5. Summary and conclusions

We have analyzed laboratory tank, wind tunnel, and field data to improve the representation of fall speeds of ice particle spanning a range of shapes and Re, with sizes from tens of microns to several centimeters, including pristine ice crystals and their aggregates through to heavily rimed particles and graupel. We find that previous analytic results used to estimate v_t appreciably underpredict the drag and overpredict the fall speed of particles where A_r is appreciably smaller than unity. Using the laboratory measurements to characterize the effect of particle shape (specifically area ratio) on C_d, we have developed an approach that improves the representation of the particle drag coefficients and terminal velocities. This approach is believed to be accurate to within 25%.

The new method collapses drag data for a wide range of A_r onto an approximately universal curve and deviations in the calculated fall speed are $<\pm 25\%$ compared to the tank data. No classification into prolate and oblate shapes is necessary [as is required for Böhm's (1989, 1992) methods], and the results work well for all area ratios from very open early aggregates through to rimed particles and graupel.

Figure 9 highlights the particle types for which Mitchell's approach fails: open particles with low area ratios, falling at low to intermediate Re. The figure shows the median percentage error in v_t calculated using Mitchell's method compared to Kajikawa's planar crystals, rosettes and side planes, and early aggregates falling in the range $\mathrm{Re} \approx 5$–200. For particles with lower area ratios the error in the computed v_t increases steadily, and these errors are significant: 60%–80% on average at $A_r = 0.2$. When the new method is applied, errors are within 30% for all A_r. This is good evidence that our new method is much more realistic for particles with open geometries.

The new approach uses the same variables as Mitchell (1996) and can therefore be applied in the same way. It is general and can be readily implemented in models. For example, it can be combined with $m(D)$ and $A(D)$ relationships from the literature (e.g., Table 1 in Mitchell 1996), or with the $A_r(D)$ relationships as a function of the normalized height within the cloud column developed by Heymsfield and Miloshevich (2003) to calculate v_t as a function of particle size and height within a cloud layer.

It is interesting to consider the consequences of this approach for aggregates. Westbrook et al. (2004) argued that the exponent b in the mass–dimensional relationship $m = aD^b$ is approximately 2.0 for snow aggregates, and this is consistent with the findings of Brown and Francis (1993), who showed that use of the coefficients $a = 0.00294$ and $b = 1.9$ (cgs units) from the Locatelli and Hobbs (1974) study for aggregates of radiating assemblages of plates, bullet rosettes, side planes, and columns as applied to particle size distributions provided

a good match with ice water content measured at the same time in cirrus clouds. Sampling through deep ice clouds during the Tropical Rainfall Measuring Mission (TRMM) Kwajalein field program yielded the relationship between area ratio and diameter of $A_r = 0.29D^{-0.18}$ (Heymsfield et al. 2002), and in deep cirrus layers $A_r = 0.18D^{-0.17}$ (Heymsfield and Miloshevich 2003). Using the new dependence of v_t on A_r, we find that the exponent β in the v_t relationship [Eq. (1)] are 0.19 and 0.25, respectively, when considered over sizes from 100 microns to 1 cm and adjusted to a surface pressure of 1000 hPa. These exponents conform well to those reported for snowfall at the ground (e.g., see Brandes et al. 2008). The exponent $\beta \approx 0$ when only large sizes above a few millimeters are considered, and this is consistent with the saturation of v_t as a function of D observed in most ground-based studies (Barthazy and Schefold 2006; Brandes et al. 2008). A key question for modeling of the aggregation process then is how rigidly the $m(D)$ and $A(D)$ relationships are followed in a natural cloud. If $v_t(D) \approx$ constant, then aggregation becomes inefficient because collisions are rare, as pointed out by Mitchell and Heymsfield (2005). But in practice it may be that the variability in $m(D)$ and $A(D)$ in the population is sufficient to drive aggregation, even if the *average* fall speed for the large particles does not vary with D (Westbrook 2005). Better measurements and characterization of the distribution of $A(D)$ and $m(D)$ are therefore vital to understand aggregation in deep systems.

Acknowledgments. We wish to thank Aaron Bansemer, Carl Schmitt, and Nick Mirsky for their help throughout the course of this project. Special thanks go to Tsuneya Takahashi and John Locatelli for providing original data. This research was supported by the JPL CloudSat Project Office, Deborah Vane, Deputy Principal Investigator, the National Science Foundation Science and Technology Center for Multiscale Modeling of Atmospheric Processes, managed by Colorado State University under Cooperative Agreement ATM-0425247, and the NASA CloudSat Project Office, NASA Award NNX07AQ85G.

CDW led the analysis of the laboratory data and this part of the study was supported by the Natural Environment Research Council, Grant NE/EO11241/1.

REFERENCES

Abraham, F. F., 1970: Functional dependence of drag coefficient of a sphere on Reynolds number. *Phys. Fluids,* **13,** 2194–2195.

Barthazy, E., and R. Schefold, 2006: Fall velocity of snowflakes of different riming degree and crystal types. *Atmos. Res.,* **82,** 391–398.

Batchelor, G. K., 1967: *An Introduction to Fluid Dynamics*. Cambridge University Press, 615 pp.

Böhm, H. P., 1989: A general equation for the terminal fall speed of solid hydrometeors. *J. Atmos. Sci.,* **46,** 2419–2427.

——, 1992: A general hydrodynamic theory for mixed-phase microphysics. I: Drag and fall speed of hydrometeors. *Atmos. Res.,* **27,** 253–274.

Brandes, E. A., K. Ikeda, G. Thompson, and M. Schönhuber, 2008: Aggregate terminal velocity/temperature relations. *J. Appl. Meteor. Climatol.,* **47,** 2729–2736.

Brown, P. R. A., and P. N. Francis, 1993: Measurements of the ice water content of cirrus using an evaporative technique. *J. Atmos. Oceanic Technol.,* **10,** 579–590.

Connolly, P. R., C. P. R. Saunders, M. W. Gallagher, K. N. Bower, M. J. Flynn, T. W. Choularton, J. Whiteway, and R. P. Lawson, 2005: Aircraft observations of the influence of electric fields on the aggregation of ice crystals. *Quart. J. Roy. Meteor. Soc.,* **131,** 1695–1712.

Field, P. R., and A. J. Heymsfield, 2003: Aggregation and scaling of ice crystal distributions. *J. Atmos. Sci.,* **60,** 544–560.

Heymsfield, A. J., and M. Kajikawa, 1987: An improved approach to calculating terminal velocities of plate-like crystals and graupel. *J. Atmos. Sci.,* **44,** 1088–1099.

——, and J. Iaquinta, 2000: Cirrus crystal terminal velocities. *J. Atmos. Sci.,* **57,** 916–938.

——, and L. M. Miloshevich, 2003: Parameterizations for the cross-sectional area and extinction of cirrus and stratiform ice cloud particles. *J. Atmos. Sci.,* **60,** 936–956.

——, A. Bansemer, P. R. Field, S. L. Durden, J. Stith, J. E. Dye, W. Hall, and T. Grainger, 2002: Observations and parameterizations of particle size distributions in deep tropical cirrus and stratiform precipitating clouds: Results from in situ observations in TRMM field campaigns. *J. Atmos. Sci.,* **59,** 3457–3491.

Hobbs, P. V., S. Chang, and J. D. Locatelli, 1974: The dimensions and aggregation of ice crystals in natural clouds. *J. Geophys. Res.,* **79,** 2199–2206.

Jayaweera, K., 1972: An equivalent disc for calculating the terminal velocities of plate-like ice crystals. *J. Atmos. Sci.,* **29,** 596–598.

——, and R. E. Cottis, 1969: Fall velocities of plate-like and columnar ice crystals. *Quart. J. Roy. Meteor. Soc.,* **95,** 703–709.

Kajikawa, M., 1971: A model experimental study on the falling velocity of ice crystals. *J. Meteor. Soc. Japan,* **49,** 367–375.

——, 1982: Observation of the falling motion of early snow flakes. Part I: Relationship between the free-fall pattern and the number and shape of component snow crystals. *J. Meteor. Soc. Japan,* **60,** 797–803.

Khvorostyanov, V. I., and J. A. Curry, 2002: Terminal velocities of droplets and crystals: Power laws with continuous parameters over the size spectrum. *J. Atmos. Sci.,* **59,** 1872–1884.

——, and ——, 2005: Fall velocities of hydrometeors in the atmosphere: Refinements to a continuous analytical power law. *J. Atmos. Sci.,* **62,** 4343–4357.

Knight, N. C., and A. J. Heymsfield, 1983: Measurement and interpretation of hailstone density and terminal velocity. *J. Atmos. Sci.,* **40,** 1510–1516.

List, R., and R. S. Schemenauer, 1971: Free-fall behavior of planar snow crystals, conical graupel and small hail. *J. Atmos. Sci.,* **28,** 110–115.

Locatelli, J. D., and P. V. Hobbs, 1974: Fall speeds and masses of solid precipitation particles. *J. Geophys. Res.,* **79,** 2185–2197.

Magono, C., and T. Nakamura, 1965: Aerodynamic studies of falling snowflakes. *J. Meteor. Soc. Japan,* **43,** 139–143.

McDonald, J. E., 1954: The shape and aerodynamics of large raindrops. *J. Meteor.,* **11,** 478–494.

Mitchell, D. L., 1996: Use of mass- and area-dimensional power laws for determining precipitation particle terminal velocities. *J. Atmos. Sci.,* **53,** 1710–1723.

——, and A. J. Heymsfield, 2005: Refinements in the treatment of ice particle terminal velocities, highlighting aggregates. *J. Atmos. Sci.,* **62,** 1637–1644.

Podzimek, J., 1965: Movement of ice particles in the atmosphere. *Proc. Int. Conf. on Cloud Physics,* Tokyo, Japan, WMO, 224–230.

Pruppacher, H. R., and J. D. Klett, 1997: *Microphysics of Clouds and Precipitation*. 2nd ed. Kluwer, 954 pp.

Rutledge, S. A., and P. V. Hobbs, 1984: The mesoscale and microscale structure and organization of clouds and precipitation in midlatitude cyclones. XII: A diagnostic modeling study of precipitation development in narrow cold-frontal rainbands. *J. Atmos. Sci.,* **41,** 2949–2972.

Stith, J. L., J. A. Hagerty, A. J. Heymsfield, and C. A. Grainger, 2004: Microphysical characteristics of tropical updrafts in clean conditions. *J. Appl. Meteor.,* **43,** 779–794.

Takahashi, T., and N. Fukuta, 1988: Supercooled cloud tunnel studies on the growth of snow crystals between −4° and −20°C. *J. Meteor. Soc. Japan,* **66,** 841–855.

——, T. Endoh, and G. Wakahama, 1991: Vapor diffusional growth of free-falling snow crystals between −3° and −23°C. *J. Meteor. Soc. Japan,* **69,** 15–30.

Tran-Cong, S., M. Gay, and E. E. Michaelides, 2004: Drag coefficients of irregularly shaped particles. *Powder Technol.,* **139,** 21–32.

Westbrook, C. D., 2005: Universality in snowflake formation. Ph.D. thesis, University of Warwick, 84 pp.

——, 2008: The fall speeds of sub-100μm ice crystals. *Quart. J. Roy. Meteor. Soc.,* **134,** 1243–1251.

——, and Coauthors, 2004: A theory of growth by differential sedimentation, with application to snowflake formation. *Phys. Rev. E,* **70,** 021403, doi:10.1103/PhysRevE.70.021403.

Wilson, D. R., and S. P. Ballard, 1999: A microphysically based precipitation scheme for the UK Meteorological Office Unified Model. *Quart. J. Roy. Meteor. Soc.,* **125,** 1607–1636.